RSC Advances

ROYAL SOCIETY OF CHEMISTRY

www.rsc.org/advances

Real-Time Release Monitoring for Water Content and Mean Particle Size of Granules in Lab-Sized Fluid-Bed Granulator by Near-Infrared Spectroscopy

Makoto Otsuka, Akira Koyama, and Yusuke Hattori

Research Institute of Pharmaceutical Sciences, Faculty of Pharmacy, Musashino University, 1-1-20 Shinmachi, Nishi-Tokyo, Tokyo 202-8585, Japan.

E-mail: motsuka@musashino-u.ac.jp

Address correspondence to:

Makoto Otsuka, Ph.D.,

Research Institute of Pharmaceutical Sciences,

Faculty of Pharmacy, Musashino University,

Shinmachi 1-1-20, Nishi-Tokyo 202-8585, Japan

Phone & Fax: 81-424-68-8658

Abstract

Simultaneous real-time monitoring of water content and mean particle size in the powder bed of a fluidized-bed granulator was performed by near-infrared (NIR) spectroscopy through a window, and the findings were used to evaluate the granular properties. A powder mixture containing acetaminophen bulk and additive powders was granulated by spraying with 10, 8.5 and 7.5% binder solutions in a lab-size fluid-bed granulator. Change of water content and mean particle size of the granules during fluid-bed granulation were evaluated by weight loss and sieving of the removed granule samples, respectively. The NIR spectra were recorded during the granulation processes, and calibration models to evaluate water content and mean particle size of the granules were developed based on NIR spectra using the partial least squares regression method. The best calibration models to predict water content and mean particle size were obtained by multiplicative scatter correction treatment. The validation results based on external validation NIR spectra also had sufficiently linear relationships. In the predicted water content-time profiles during the granulation processes, the water content increased in the granulation process, and it decreased in the drying process; the predicted values fitted very well to the actual values in all processes. The maximum water content in the processes using 8.5 and 7.5% binder solutions was around 6-7%,

but that using 10% binder solution was around 3%. In terms of the predicted mean particle size-time profiles, they increased during the granulation process, remained constant during the drying process; the predicted profile fitted very well to the actual values in all processes.

Keywords: Real-time monitoring; process analytical technology; water content; mean particle size; reflectance near-infrared spectroscopy; fluidized-bed granulator; chemometrics

Introduction

Since controlling of wetting and drying of pharmaceutical powder solids is conventional and frequent operation in the practical manufacturing processes, solid-water interaction is one of the fundamental issues in pharmaceutical technology.[1] The state of water in solid dosage forms may be characterized using X-ray diffraction, microscopic methods, thermal analysis, vibrational spectroscopy and nuclear magnetic resonance spectroscopy.[2] In the pharmaceutical industry, wet granulation is generally carried out with water to improve the physical properties of raw powdered materials, such as the powder flow, compression properties, increasing the density, ensuring mixture uniformity and reducing the dust.[3] Additionally, the water content during granulation processes affects the pharmaceutical properties of final products, such as polymorphic crystalline stability, drug degradation rate and drug release rate.

Fluid-bed granulation is a popular wet granulation technique for producing granules in the pharmaceutical industry by spraying a binder solution onto a fluidized powder. The control of fluidized-bed granulation has been carried out by on indirect measurements of the amount of air, moisture content, amount of powder solids, their temperature and their mass-balance calculation.[4-6]

On the other hand, regulatory authorities such as the US Food and Drug Administration and the International Conference on Harmonization have promoted and requested real-time control of drug product quality and the application of quality-by-design principles using in-line analytical tools, as process analytical technology (PAT).[7-8] Since the introduction of FDA guidelines for PAT, in-line real-time analysis as a tool to monitor and control manufacturing processes has become increasingly accepted in the pharmaceutical industry.[9-10]

The nondestructive character of vibrational spectroscopy techniques, such as near-infrared spectroscopy (NIR), makes them a novel tool for in-line quality assurance as PAT,[11-13] since the development of PAT will provide an in-line window on the physicochemical phenomena occurring during pharmaceutical manufacture. NIR can be applied for both quantitative analysis of water[14-15] and determining the state of water in solid materials[16-17] during granulation. This enables us to understand the molecular level phenomena during manufacture of pharmaceutics. Further more, NIR has been applied to study the nature of water-solid interactions within various materials.[18] Several authors have reported the monitoring of moisture levels using NIR in a fluid bed.[19] Rantanen et al. described[20-21] the real-time monitoring of moisture using of NIR for process monitoring and control during fluid-bed granulation and drying.

Peinado et al.[21] developed a calibration model to predict water content, and validated and transferred an NIR model to determine the end-point for commercial production batches of an FDA-approved solid oral product. Rantanen et al.[23-24] have demonstrated the use of multivariate NIR chemometric models coupled with temperature and humidity data recorded by the data loggers to develop models for better understanding of the fluid-bed granulation process. However, there is no report on a simultaneous real-time release monitoring pharmaceutical properties, such as water content and mean particle size, of granules during fluidized bed granulator by using NIR.

This is the first study of simultaneous prediction of the water content and the mean particle size of conventional granules in a lab-sized fluid-bed granulator by in-line NIR monitoring. Pharmaceutical properties of the granules depended on the binder solution concentration and changes of water content and mean particle size of the granules obtained using different binder solutions were evaluated using a chemometric method.

Materials and Methods

Materials

Bulk powder of acetaminophen (Lot No. 90197) was obtained from Iwaki Pharm. Co. Ltd. Diluents, α-lactose monohydrate (Pharmatose 200M, Lot 30330-2175), was obtained from DFE Pharm (Amsterdam, Holland). A binder, hydroxyl-propyl-cellulose (Nisso HPC-L, Lot No. NHB-4811), was obtained from Nippon Soda Co. Ltd. (Tokyo, Japan). A lubricant, magnesium stearate (Lot No. SDF1110, derived from a natural plant), was obtained from Wako Chemical Co. Ltd. (Tokyo, Japan).

Preparation of granules

The powder mixture consisted of bulk powders of acetaminophen (30.8 g), crystalline α-lactose monohydrate (188.4 g), and microcrystalline cellulose (80.8 g), as shown in Table 1. Figure 1 shows the lab-sized fluid-bed granulator (Okada Seiko, Ltd., Tokyo, Japan) with a chamber (160 mm in diameter and 6.0 L in volume) made of glass used to prepare granules. A sampling port was equipped at 3-cm from the bottom of a chamber of the granulator, and granular samples was withdrawn by a plastic sampling bar in diameter 15 mm. The granulator was loaded with a reflectance NIR spectrometer, and NIR light focused on at 3 cm from the bottom and center of the chamber to measure granular properties during granulation. The binder solutions (10, 8.5 and 7.5%) of hydroxypropyl cellulose (7.9 g) were prepared to be dissolved in different amounts of water (71.1 g, 85.1 g and 97.1 g). Fluid-bed operation conditions

were fixed during all processes as follows: warming up time was 20 min at 35°C, rotor speed was 360 rpm and spray down occurred at 200 mm height from the bottom mesh screen with an air spray presser, at 0.1 MPa. The spray speeds for 10, 8.5 and 7.5% binder solutions were at 3.95, 4.64 and 5.26 g/min, respectively, as shown in Table 2. The powder mixture (307.9 g) containing the bulk and additives powders was agitated and mixed at 35±2°C in the chamber for 5 min, and then the binder solutions were sprayed into the powder mixture at 35±2°C for 20 min, which was then dried at 60±2°C for 10 min. The wet-granular powder samples (1.0 g) were withdrawn from the chamber at predetermined intervals (every 3 minutes), with 12 granular samples obtained in each experiment (the binder solutions, 10, 8.5 and 7.5%), and the total was 36 samples.

Granular properties of the samples

The sample granules in glass containers were dried in a hot air oven at 70±2°C for 24 hours, and then, the loss due to drying was measured using their weight. The dried granular samples were passed through six kinds of mesh sieve screen (75, 106, 150, 355, 500 and 850 μm), and the weights of sieved granular sample fractions were measured to evaluate mean particle sizes. The mean particle size (D50) was evaluated as median particle size by 50% cumulative weight of the sieved fractions.

Microscopic observation of the granules:

Microscopic observation of the granular samples was performed by digital microscopy (Type VHX-100, Keyence Co. Ltd., Tokyo, Japan) and scanning electron microscopy (SEM) (JSM-6510LV, Jeol Co. Ltd., Tokyo, Japan), respectively.

NIR spectroscopic measurements

The NIR reflectance spectra for raw powder materials were recorded over the range of 12000-4000 cm^{-1} (32 scans with 8 cm^{-1} resolution) using an NIR spectrometer (MPA, Bruker Optics, Ettlingen, Germany). Another NIR spectrometer (MATRIX-F, Bruker Optics, Ettlingen, Germany) was set in front of the fluid bed with a focal length of 250 mm. NIR reflectance spectra were measured through a glass wall, and recorded 10 times every minute with scan time, 10 scans/spectrum; resolution, 64 cm^{-1} and wavelength range, 12000-4000 cm^{-1} during all granulation processes. In order to measure accurate spectra during granulation, the wall of the fluid-bed granulator was periodically percussed using a rubber spatula for keeping clean glass wall.

Partial Least Squares (PLS) Model: The water content and D50 of the standard granule samples for calibration models were estimated with a PLS model. The granulation experiments were performed with three kinds of binder solution (10, 8.5 and 7.5% HPC) for 35 minutes, the NIR spectra were measured six times at every sample

collect on time (12 samples x 3 kinds of the solution), and a total of 216 spectra were measured. Then, 108 NIR spectra were randomly selected to prepare the calibration models to predict water content and D50. The other 108 spectra were used as an external validation data set for validation testing. The best calibration model was determined to minimize the standard error of cross-validation (SEV) by the leave-one-out method in PLS regression software, after the spectral data were transformed by various functions, such as non-treatment (NON), area normalized (NOR), second derivative (2nd), standard normal variate (SNV) and multiplicative scatter correction (MSC). Cumulative percent variance (CV), Prediction Residual Error Sum of Squares (PRESS) and the r-values for calibration and validation (r-Cal and r-Val) were evaluated as shown below, and the calculated chemometric parameters are summarized in Table 3.

When cross-validation was applied during PLS, a regression model for a validation sample x_v was evaluated based on k factor regression vector β_k.[25]

$$\hat{y}_v = x_v \beta_v \quad (1)$$

Then, the prediction residual can be generated

$$\hat{f} = y_v - \hat{y}_v, \quad (2)$$

where y_v is the "true" value for the dependent variable of the validation sample.

To keep the notation simple, hatted symbols indicate a k factor estimate of a quantity.

For a set of n_v validation samples, a Prediction Residual Error Sum of Squares (PRESS) can be calculated for the y block:

$$PRESS = f^T f \quad (3)$$

Related to the PRESS is the Standard Error of Prediction (SEP), which takes into account the number of samples and has the same units as the y variable.[25]

$$SEP = \sqrt{\frac{PRESS}{n_v}} \quad (4)$$

The most naive version of validation predicts on the basis of training set samples. This type of SEP is termed a Standard Error of Calibration (SEC). The SEC must be corrected for the number of factors k in the model:

$$SEC = \sqrt{\frac{PRESS}{n_v - k}}, \quad (5)$$

On the other hand, the other 108 spectra of the external validation data set were used to validate the best fitted calibration models for water content and D50. The validated chemometric parameters of the best calibration models are summarized in Table 4. The analysis was performed using the chemometric software Pirouette version 3.11 (InfoMetrix, Inc., Bothel, WA, USA).

All granulation processes in a fluid-bed granulator were monitored for 35 min by reflectance NIR spectroscopy and 245 NIR spectra were obtained. The granular samples were obtained with three kinds of binder concentration solution, and the water content and D50 of the granules were predicted based on 735 spectra by the best calibration models.

Results and Discussion

Change of NIR spectra of acetaminophen granular formulation during fluid-bed granulation process

Figure 2 shows NIR spectra for raw powder materials. The NIR spectral peaks of the raw materials were identified based on a reported database[26] as follows: The NIR spectrum of acetaminophen bulk powder had specific peaks at 4069 cm^{-1} due to CH stretching (st) and CC st, 4335 cm^{-1} due to NH st and C=O st in a CONH group, at 4667 cm^{-1} due to CH st and deformation (DF) in a CH_2 subscript group, at 4944 cm^{-1} due to C=O st 2nd overtone (OT) in a CONH group, at 6013 cm^{-1} due to CH st 1st OT in an aromatic ring and 8836 cm^{-1} due to CH st 2nd OT in an aromatic ring. The spectrum of MCC had specific peaks at 4775 cm^{-1} due to 2nd OT and DF of CH st in a CH_2 group, 5218 cm^{-1} due to 1st OT of OH st and 6700-6800 cm^{-1} due to 1st OT of OH st. The

spectrum of α-lactose monohydrate had specific peaks at 4775 cm^{-1} due to 2nd OT and DF of CH st in a CH_2 group, 5218 cm^{-1} due to 1st OT of OH st and 6300-6700 cm^{-1} due to 1st OT of OH st. The spectrum of HPC had specific peaks at 4775 cm^{-1} due to 2nd OT and DF of CH st in a CH_2 group, 5218 cm^{-1} due to 1st OT of OH st, 5843 cm^{-1} due to 1st OT of CH st of CH_3 in a propyl group, 6700-7000 cm^{-1} due to 1st OT of OH st and at 8500-8600 cm^{-1} due to 2nd OT CH st of CH_3 in a propyl group.

Figure 3 shows the change of MSC-corrected NIR spectra of the powder sample with 10% HPC binder solution during the fluid-bed granulation process. In the mixing process for 5 min, NIR spectra were not significantly changed as determined by visual observation. In the granulation process for 5-25 min, the whole NIR spectral intensity increased with an increase of the sprayed binder solution amount, meaning that the granular size increased with an increase of the binder solution amount. In the final drying process for 25-35 min, the absorption peak at around 5200 cm^{-1} due to free water decreased over time due to drying of water in the granules.

<u>Development of calibration models to predict water content and D50 of the granules</u>

Pharmaceutical properties of fluid-bed granules, such as mean particle size, particle size distribution, porosity and granular strength, might differ among batches based on

granulation conditions, such as binder solution conditions, agitation rate, temperature and amount of air. The calibration models to evaluate water content and D50 of the granules during the granulation process were, therefore, developed based on 108 NIR spectra by using the PLS method involving various pre-treatment functions.

Table 3 shows the effect of pre-treatments on chemometric parameters to predict water content and D50 of the granules obtained by fluid-bed granulation with various binder concentration solutions. The result indicated that the minimum SEV value by the leave-one-out method could thus be realized by using the best calibration model for the analysis of NIR spectra after suitable pre-treatment. The orders of SEV for calibration models to predict water content and D50 were MSC<SNV<2nd<NOR<NON and MSC<NOR<2nd<SNV<NON, respectively. The best calibration models to predict water content and D50 were by MSC treatment, and consisted of 5 and 8 principal components involving 98 and 99% cumulative variance, respectively. Additionally, the results of r-Val and PRESS-Val evaluated by the leave-one-out method also supported the assertion that the best calibration models were by MSC.

Finally, the orders of SEC for the calibration models to predict water content and D50 were MSC<SNV<2nd<NOR<NON and MSC<NOR<2nd<SNV<NON, and the PRESS-Cal had almost the same tendency. The r-Cal of the models to predict water

content and D50 were 0.9903 and 0.9613, respectively, indicating that the best calibration models for water content and D50 were by MSC.

Validation of the best fitted calibration models

To validate the created PLS calibration models to predict water content and D50 of the granules, the other 108 NIR spectra as an external validation set were applied to each calibration model. The PRESS and SEP of the calibration models were calculated based on the external validation data sets and are summarized in Table 4. The SEP values for water content and D50 of the granules obtained by MSC pretreatments were sufficiently small.

Figure 4 shows the relationships between predicted and actual water content and D50 of the granules based on validation NIR spectral data sets by the best calibration model. The plots for water content and D50 gave a straight line (r-Val were 0.9903 and 0.9613) with slopes of 0.9807 and 0.9241 and *Y*-intercepts of 0.046% and 13.61 μm, indicating that the best calibration models by MSC had a significantly linear relationship with high repeatability.

<u>Science background of PLS calibration models to predict pharmaceutical properties of</u>

the granules

PLS regression is effective in extraction of feature and regularity, and modeling of the large numerical data. However, the disadvantages of PLS regression are the difficulty of interpretation of the factors, and that it is necessary to determine the number of factors to be used. Therefore, in order to prove the validity of the PLS models to predict the water content and D50, were examined for evidence of the regression vectors, respectively.

Figure 5-(a) shows that the regression vector for water content had positive peaks at 4998 cm^{-1} due to OH st bonded, at 5276 cm^{-1} due to OH st free water, at 7004 cm^{-1} due to OH st 1st OT, and at 11,500 cm^{-1} due to CH st 3rd OT. In contrast, the negative peaks were at 4289 cm^{-1} due to CH st and CH df and at 4690 cm^{-1} due to NH st 2nd OT. All positive peaks were related to hydrophilic groups such as OH group or free water, since the water interacted with hydrophilic functional groups, so it seemed that the peak intensity of hydrophobic groups was comparatively decreased.

On the other hand, Figure 5-(b) shows that the regression vector for D50 had positive peaks at 4350 cm^{-1} due to NH st, at 6788 cm^{-1} due to NH st 1st OT and at 8824 cm^{-1} due to CH st 2nd OT. The negative peaks were at 4227 cm^{-1} due to CH df 2nd OT, at 4998

cm^{-1} due to OH st bonded, at 6109 cm^{-1} due to CH st 1st OT, at 7775 cm^{-1} due to CH st 2nd OT and at 9534 cm^{-1} due to CHdf 2nd OT.

The vector for D50 indicated that both positive and negative peaks were not significantly related to the peaks due to an OH group. The peaks in the vector did not match the peaks in the actual NIR profiles, meaning that the peaks in the vector were related to the baseline shifting. It is well known that physical information of particle size reflects the NIR baseline, and there is a linear relationship between height of the baseline and particle size.[27]

Figure 6 shows the loading vectors of calibration models for water content and D50 of the granules. In the loadings for water content (Figure 6-a), the PC1 had a positive peak at 5214 cm^{-1} due to OH st and free water, and at 7096 cm^{-1} due to OH st 1st OT, but the PC2 had positive peaks at 6017 cm^{-1} due to CH st of 1st OT and at 8810cm^{-1} due to CH st of 2nd OT, meaning that the PC1 loading was due to free water and the PC2 was similar to acetaminophen. Since the percent vaiances for PC1 and PC2 were 76.3 and 9.42%, respectively, PC1 due to additive water was a major component. In contrast, PC2 was due to the other functional chemical groups of acetaminophen, which were a minor component.

In the loadings for the D50 (Figure 6-b), the PC1 also had positive peaks at 5245 cm^{-1} due to OH st, and free water, and at 7066 cm^{-1} due to OH st 1st OT, but the PC2 had positive peaks at 5986 cm^{-1} due to CH st of 1st OT and at 8810cm^{-1} due to CH st of 2nd OT, and a negative peak at 5183 cm^{-1} due to OH st bonded. Since the percent variances for PC1 and PC2 were 62.2 and 21.8%, respectively, the PC1 and PC2 loading might be due to free water and interaction peaks with the other functional chemical groups of acetaminophen, respectively. The particle size of the granules increased in proportion to the additive water amount, but their contribution in the loading vector for the calibration model was not so great, as shown by the percent variance of PC1 and PC2.

Figure 7 shows the relationships between PC1 and PC2 for water content and D50 of the granules. In the score plot profiles to predict the water content and D50, PC1 and PC2 indicated the amount of free water and the other chemical functional groups of API, as shown in the result of loading vectors in Figure 6. The profiles for D50 significantly depended on the amount of water in binder solutions.

<u>Prediction of water content and D50 of the granules during fluid-bed granulation process</u>

Figure 8-a shows the predicted water content-time profiles during all fluid-bed granulation processes; the water content increased during the granulation process and it decreased during the drying process. The predicted water contents fitted very well to actual values of sampling granules in all processes. The maximum water content in the processes using 8.5 and 7.5% binder solutions was around 6-7%, but that using 10% binder solution was around 3%. Total amount of water added for the 7.5%, 8.5% and 10% of binder solutions was approximately 24%, 22% and 19% of the total weight respectively and differ only slightly. However, the water content for 10% of binder solution was almost half and significantly small compared to the other solutions. Drying rate of binder solution was inverse proportion with their concentration, since viscosity of polymer solution was proportional with their concentrations; therefore, drying rate for 10% HPC granulation is slower than the others. This result indicated that the maximum water contents depended on a balance of spraying and drying rates of water in the fluid-bed chamber, and affected the viscosity of the binder solution.

Figure 8-b shows the predicted D50-time profiles; the D50 increased during the granulation process and then remained constant during the drying process. The predicted D50 profile fitted very well to the actual values of sampling granules in all processes. The result indicated that the final D50 of granules increased with

decreasing binder concentration and/or increasing of spray speed. Total amount of water added for the 7.5%, 8.5% and 10% is approximately 24%, 22% and 19% of the total weight respectively and differ only slightly. However, the water content for 10% binder concentration is significantly small (almost half) compared to the other concentrations. Can the authors elaborate on the possible reason/explanation for this finding.

Figure 9 shows visual observation of the powder samples during granulation using 10% HPC solution. In the sample for 5 min, powder particles of less than 20 μm in diameter were observed, and the powder was aggregated and formed wet-granules of 50-200 μm in diameter for 16 min, and then the samples for 35 min were granules of 100-250 μm in diameter.

Figure 10 shows the SEM observations of the granules obtained with 7.5, 8.5 and 10% HPC solutions. The granules obtained using 10% HPC solution had more irregular surfaces and particle shapes with a wide particle size distribution, while those using 7.5 and 8.5% HPC solutions (water- rich solutions) had smooth surfaces and a narrow particle size distribution.

Conclusion

The present study demonstrated the possibility of using NIR spectroscopy to predict the water content and D50 of acetaminophen formulation granules during mixing, granulation and drying processes in a laboratory-sized fluid-bed granulator. Binder solution concentration might be used to control the size of the granules. Accurate calibration models to predict water content and D50 were established, and their chemometric parameters exhibited chemical interaction between additive water and powder solids. Since this technique provides better understanding and monitoring of fluid-bed granulation, real-time release monitoring of fluid-bed granulation by NIR very important for product quality.

Acknowledgement

The authors wish to thank Mr. Takashi Sato, *CAMO Software Japan Co. Ltd.* for technical advice on the chemometrics.

Declaration of interest: Supported by Grants from Musashino Joshi-Gakuin.

References

1. G. Zografi States of water associated with solids. *Drug Dev Ind Pharm.* 1988, 14, 1905-1926.

2. H. Brittain, Methods for the characterization of polymorphs and solvates. In: H. Brittain, ed. Polymorphism in pharmaceutical solids. 1st ed. New York: Marcel Dekker Inc, 1999, 227-278.

3. S.L. Cantor, L.L. Augsburger, S.W. Hoag, A.H. Gerhardt, Wet Granulation. In: Hoag, S.W., Augsburger, L.L. (Eds.), Pharmaceutical Dosage Forms: Tablets Volume I., Third Edn., 2008, Informa Healthcare, New York.

4. T. Schaefer, O. Wørt, Control of fluidized bed granulation III. Effect of inlet air temperature and liquid flow rate on granule size and size distribution, Control of moisture content of granules in the drying phase. *Arch Pharm Chem Sci.* 1978, 6, 1-13.

5. T. Abberger, J. Raneburger, H. Egermann, Instrumentation of laboratory-scale fluid-bed granulator for critical moisture content and of free moisture. *Sci Pharm.* 1996, 64, 255-262.

6. K. Wöstheinrich, P. Schmidt, Evaluation and validation of a fully instrumented Hüttlin HKC 05-TJ laboratory-scale fluidized bed granulator, *Drug Dev Ind Pharm.* 2000, 26, 621-633.

7. "Process Analytical Technology (PAT) Initiative", U.S. Food and Drug Administration Center for Drug Evaluation and Research Home Page (http://www.fda.gov/AboutFDA/CentersOffices/OfficeofMedicalProducts andTobacco/CDER/ucm088828.htm).

8. "International Conference on Harmonization of Technical Requirements for Registration of Pharmaceuticals for Human Use. Pharmaceutical Development Q8 (R2) ". Accessed August 2009, at: http://www.fda.gov/downloads/Drugs/ GuidanceComplianceRegulatoryinformation/Guidances/ ucm073507.pdf.

9. L.X. Yu, Pharmaceutical quality by design product and process development, understanding and control, *Pharm. Res.* 25 (10), 781–791 (2008).

10. T. De Beer, A. Burggraeve, M. Fonteyne, L. Saerens, J.P. Remon and C. Vervaet, Near infrared and Raman spectroscopy for the in-process monitoring of pharmaceutical production processes, *Int. J. Pharm*, 2011, 417(1-2), 32–47.

11. K. R. Beebe , W. W. Blaser, R. A. Bredeweg, J. Paul Chauvel Jr., R. S. Harner, M. LaPack , A. Leugers , D. P. Martin, L. G. Wright, E. Deniz Yalvac, Process analytical chemistry. *Anal Chem.* 1993, 65, 199R-216R.

12. J. Workman, A review of process near infrared spectroscopy: 1980-1994. *J Near Infrared Spectrosc.* 1993, 1, 221-245.

13. T. Axon, R. Brown, S. Hammond, S. Maris, F. Ting, Focusing near infrared spectroscopy on the business objectives of modern pharmaceutical production. *J Near Infrared Spectrosc.* 1998, 6, A13-A19.

14. P. Frake, D. Greenhalgh, S. Grierson, J. Hempenstall, D. Rudd, Process control and end-point determination of a fluid bed granulation by application of near infra-red spectroscopy. *Int J Pharm.* 1997, 151, 75-80.

15. J. Rantanen, S. Lehtola, P. Rämet, J.P. Mannermaa, J. Yliruusi, On-line monitoring of moisture content in an instrumented fluidized bed granulator with a multichannel NIR moisture sensor. *Powder Technol.* 1998, 99, 163-170.

16. P. Luukkonen, J. Rantanen, K. Mäkelä, E. Räsänen, J. Tenhunen, J. Yliruusi, Characterization of silicified microcrystalline cellulose and a-lactose monohydrate wet masses using near infrared spectroscopy. *Pharm Dev Technol.* 2001, 6, 1-9.

17. E. Räsänen, J. Rantanen, A. Jørgensen, M. Karjalainen, T. Paakkari, J. Yliruusi, Novel identification of pseudopolymorphic changes of theophylline during wet granulation using near infrared spectroscopy. *J Pharm Sci.* 2001, 90, 389-396.

18. S. Delwiche, R. Pitt, K. Norris, Examination of starch-water and cellulose-water interactions with near infrared (NIR) diffuse reflectance spectroscopy. *Starch/Stärke.* 1991, 43, 415-422.

19. N. Heigla, D. M. Kollera, B. J. Glasserb, F. J. Muzziob, J. G. Khinasta, Quantitative on-line vs. off-line NIR analysis of fluidized bed drying with consideration of the spectral background, *European Journal of Pharmaceutics and Biopharmaceutics,* 2013, 85(3), Part B, 1064–1074.

20. J. Rantanen, O. Antikainen, J.P. Mannermaa, J. Yliruusi, Use of the near-infrared reflectance method for measurement of moisture content during granulation. Pharm. Dev. Technol. 2000a, 5, 209–217, http://dx.doi.org/ 10.1081/PDT-100100536.

21. J. Rantanen, A. Jørgensen, E. Räsänen, P. Luukkonen, S. Airaksinen, J. Raiman, K. Hänninen, O. Antikainen, J. Yliruusi, Process analysis of fluidized bed granulation. *AAPS PharmSciTech* 2001, 2, 21, http://dx.doi.org/10.1208/pt020421.

22. A. Peinado, J. Hammond, A. Scott, Development, validation and transfer of a near infrared method to determine in-line the end point of a fluidised drying process for commercial production batches of an approved oral solid dose pharmaceutical product. *J. Pharm. Biomed. Anal.* 2011, 54, 13–20, http://dx.doi.org/10.1016/j.jpba.2010.07.036.

23. J. Rantanen, M. Knskoski, J. Suhonen, J. Tenhunen, S. Lehtonen, T. Rajalahti, J.P. Mannermaa, J. Yliruusi, Next generation fluidized bed granulator automation. *AAPS PharmSciTech*, 2000b, 1, E10, http://dx.doi.org/10.1208/pt010210.

24. Rantanen, J., Jørgensen, A., Räsänen, E., Luukkonen, P., Airaksinen, S., Raiman, J.,

Hänninen, K., Antikainen, O., Yliruusi, J., 2001. Process analysis of fluidized bed granulation. AAPS PharmSciTech 2, 21, http://dx.doi.org/10.1208/pt020421.

25. Software manual for Pirouette Ver. 3.11 (Infometrix Co., Woodenville WA).

26. M. Iwamoto, S. Kawano, J. Uozumi, Introduction of Near Infrared Spectroscopy, Sachi Syobou Co., 1994.

27. M. Otsuka, Comparative Particle Size Determination of Phenacetin Bulk Powder by Using Kubelka-Munk Theory and Principle Component Regression Analysis Based on Near-Infrared Spectroscopy, *Powder Tech.,* 2004, 141, 244-250.

Figure captions.

Figure 1. Lab-sized fluid-bed granulator equipped with reflectance NIR spectroscopy.

Figure 2. NIR spectra of raw powder materials.

Figure 3. Change of NIR spectra during granulation processes in fluid-bed granulator.

Figure 4. Development of calibration model to predict water content and D50 by PLS.

Figure 5. Change of NIR spectra and RV during granulation process.

Figure 6. Loadings of PC1 and PC2 of granulation process.

Figure 7. Change of PC1 and PC2 scores during granulation.

Figure 8. Predicted water content and D50 during granulation processes.

Figure 9. Visible observation of fluid-bed granulation process with 10% HPC solution.

Figure 10. SEM observation of fluid-bed granules obtained using 7.5, 8.5 and 10% HPC solutions.

Table 1. Granular formulation for fluid-bed granulation.

Table 2. Spray conditions for fluid-bed granulation.

Table 3. Chemometric parameters to predict water content and D50 by PLS in fluid-bed granulation process.

Table 4. Validation result for the best calibration models to predict water content and D50 by PLS in fluid-bed granulation process.

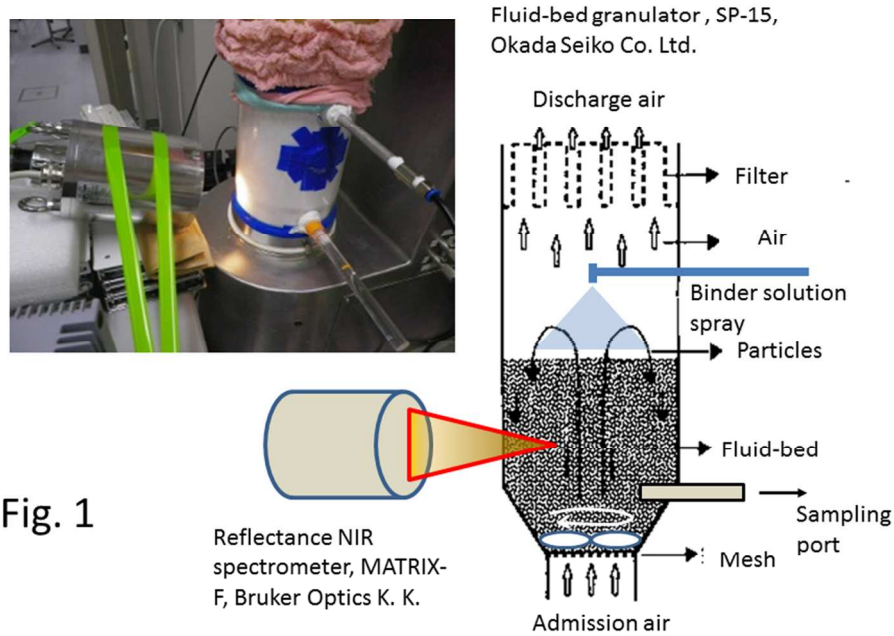

Fig. 1

254x190mm (96 x 96 DPI)

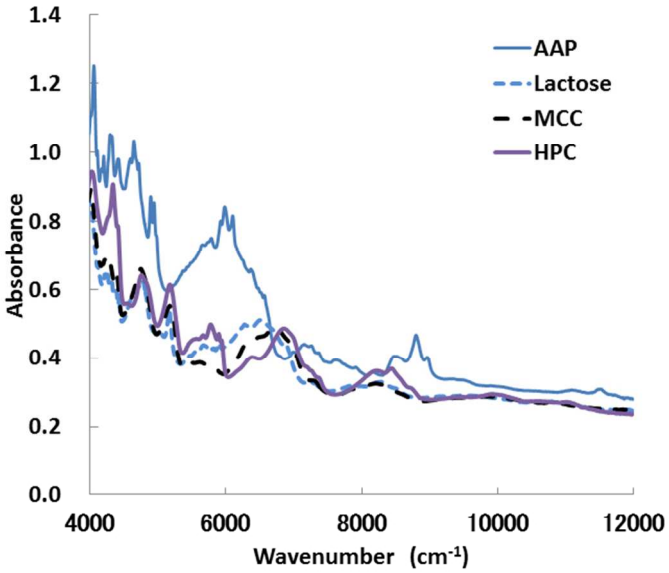

Fig. 2.

254x190mm (96 x 96 DPI)

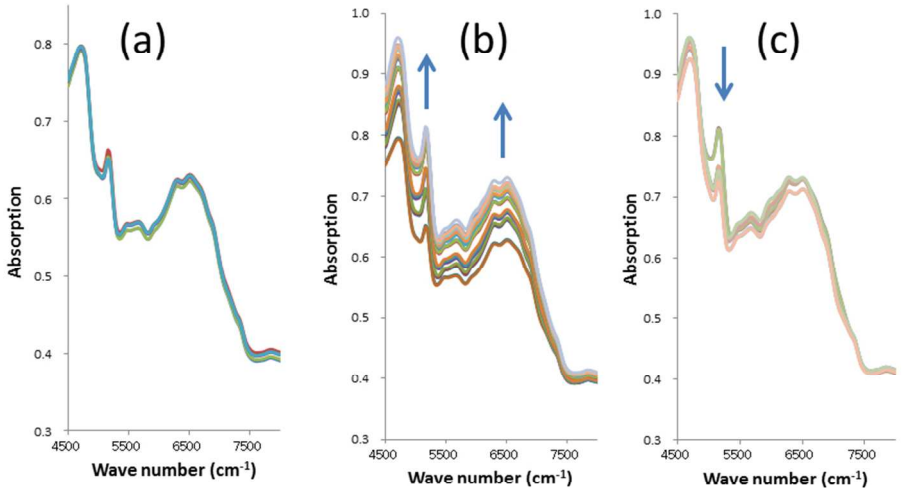

Mixing process For 0-5 min

Granulation process For 5-25 min

Drying process For 25-35 min

Fig. 3

254x190mm (96 x 96 DPI)

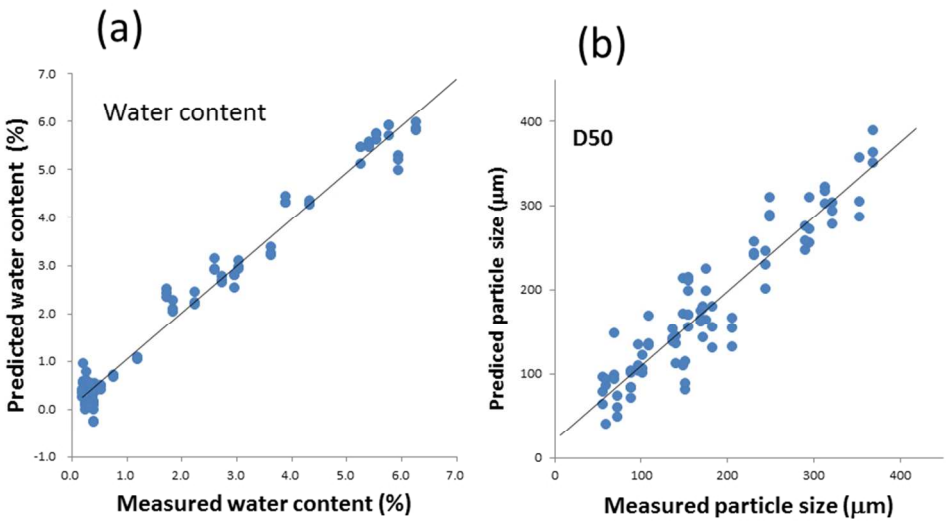

Fig. 4.

254x190mm (96 x 96 DPI)

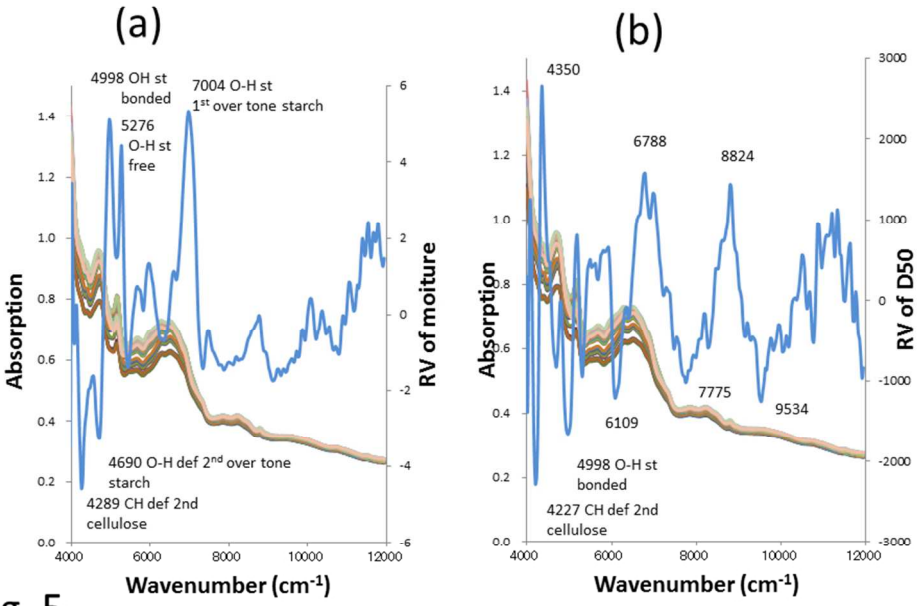

Fig. 5.

254x190mm (96 x 96 DPI)

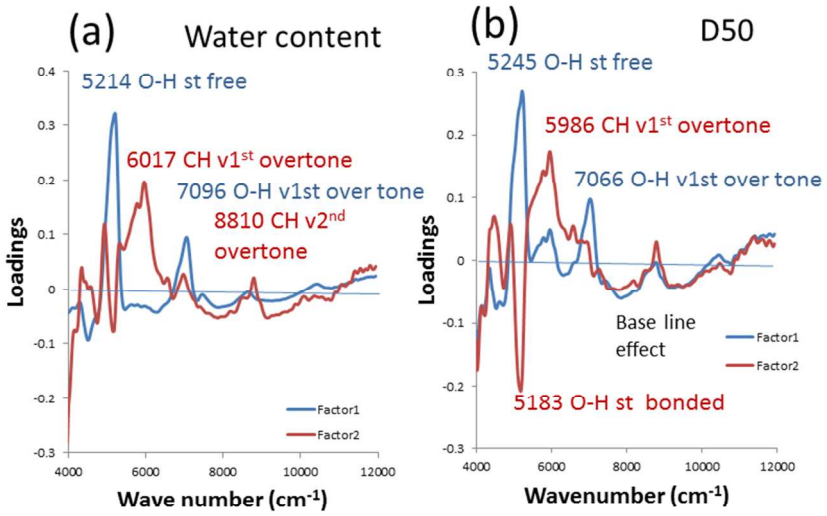

Fig. 6.

254x190mm (96 x 96 DPI)

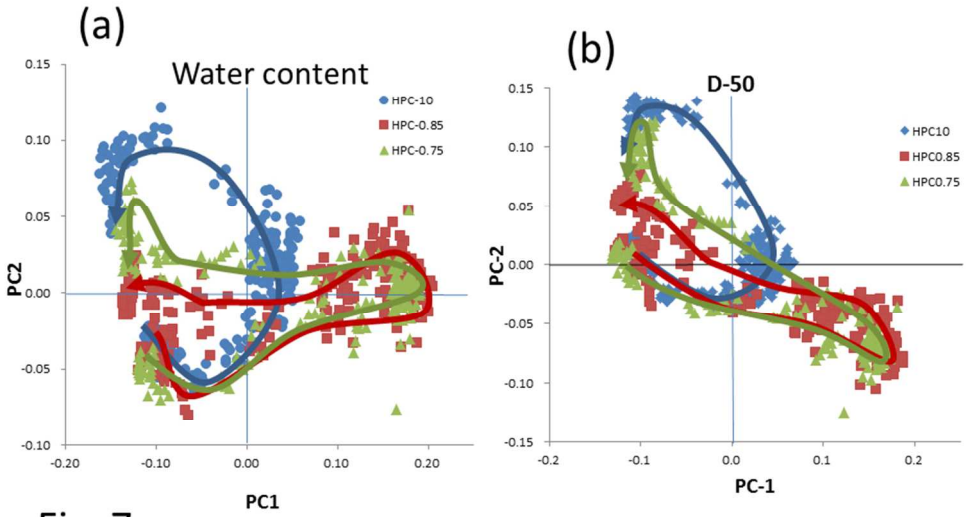

Fig. 7.

254x190mm (96 x 96 DPI)

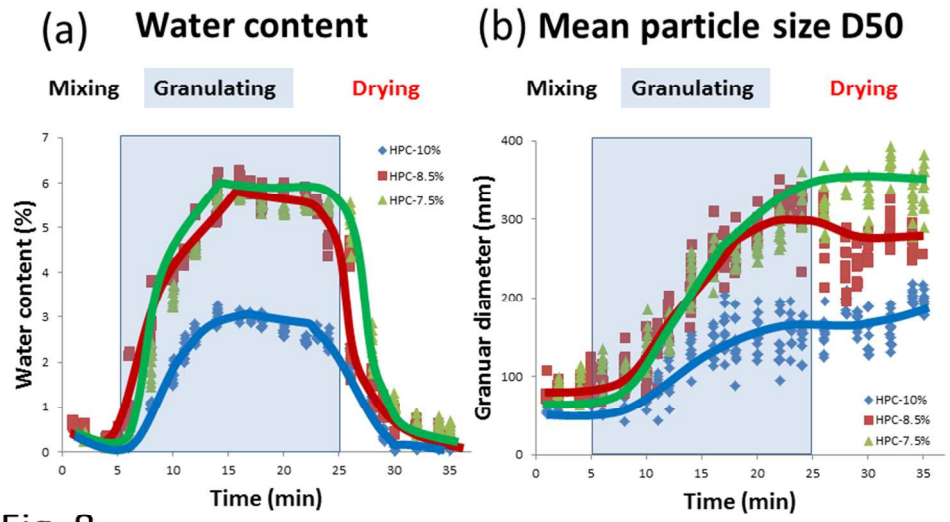

Fig. 8.

254x190mm (96 x 96 DPI)

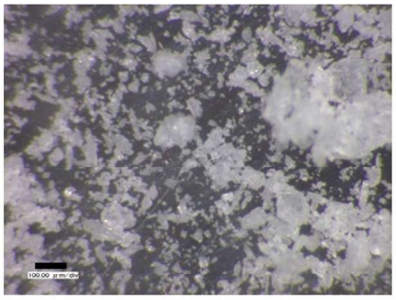

After granulation for 1 min (mixing process).

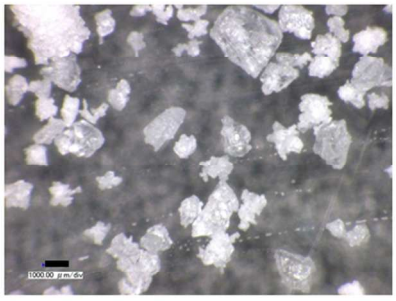

After for 16 min (granulation process).

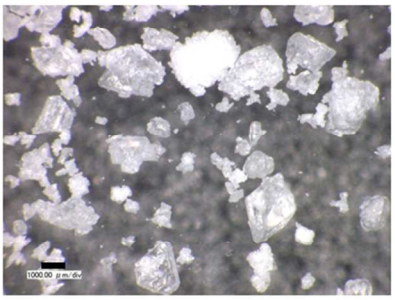

After for 35 min (drying process).

Fig. 9.(HPC 10%)

254x190mm (96 x 96 DPI)

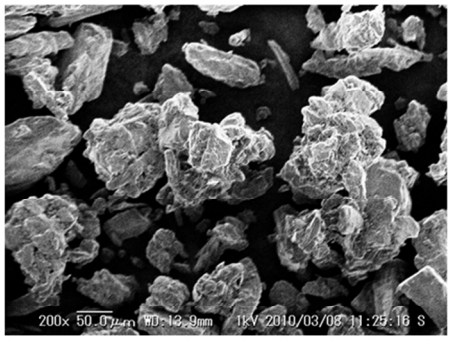

10%HPC

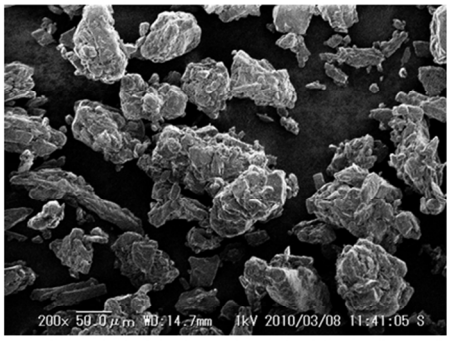

8.5%HPC

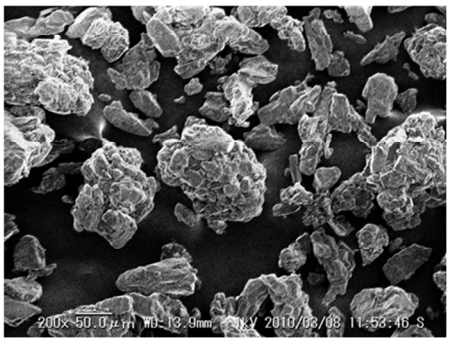

7.5%HPC

Fig. 10.

254x190mm (96 x 96 DPI)

Table 1. Lab-sized formulation.

	Composition amount (g)	Composition rate (%)
Acetaminophen (AAP)	30.8	10
Crystalline α-lactose monohydrate (Lactose)	188.4	61
Microcrystalline cellulose (MCC)	80.8	26
Hydroxypropyl cellulose (HPC)	7.9	3
Total	307.9	100

254x190mm (96 x 96 DPI)

Table 2. Spray conditions of granulation.

	10 %HPC	8.5 %HPC	7.5 %HPC
Binder solution additives(g)	79	93	105
HPC additives(g)	7.9	7.9	7.9
Water additives(g)	71.1	85.1	97.1
Spray speed(g/min)	3.95	4.64	5.26
Spray time(min)	20	20	20

254x190mm (96 x 96 DPI)

Table 3.

Moist content								
Function	Factors	CV	SEV	Press Val	r Val	SEC	Press Cal	r Cal
Non	3	99.70	0.4412	1.694E+01	0.9774	0.4218	1.476E+01	0.9803
MSC	5	97.92	0.3259	9.242E+00	0.9877	0.2996	7.272E+00	0.9903
2nd	4	99.33	0.4034	1.416E+01	0.9811	0.3756	1.157E+01	0.9846
Nor	3	98.81	0.4260	1.579E+01	0.9789	0.3955	1.298E+01	0.9827
SNV	4	96.32	0.3388	9.987E+00	0.9867	0.3167	8.224E+00	0.9891
D50								
Function	Factors	CV	SEV	Press Val	r Val	SEC	Press Cal	r Cal
Non	1	76.30	72.35	4.554E+05	0.6185	66.71	3.782E+05	0.6820
MSC	8	98.99	32.19	9.016E+04	0.9341	26.22	5.362E+04	0.9613
2nd	7	99.74	34.20	1.018E+05	0.9253	27.66	6.045E+04	0.9563
Nor	8	99.84	37.57	1.228E+05	0.9114	27.64	5.958E+04	0.9569
SNV	7	99.74	34.20	1.018E+05	0.9253	27.66	6.045E+04	0.9563

254x190mm (96 x 96 DPI)

Table 4.

	Water content	D50
SEP	2.891E-01	2.483E+01
PRESS	7.272E+00	5.362E+04
r	0.9903	0.9613
Factors	5	8
Slope	0.9808	0.9242
Intercept	4.569E-02	1.361E+01
ModelESS	3.750E-02	1.986E-02

254x190mm (96 x 96 DPI)